

changes in particle diffusivity do not explain the trends shown in Figure 6, in which earlier cycles exhibit greater degrees of induction and/or acceleration in the hydration conversion-time curve. In addition, a mechanism based solely on differences in diffusion coefficient provides no explanations for the similar manner of porosity change with conversion in rapidly hydrating solids, in spite of very different preparation history (Figures 9 and 10), nor for the quite different porosity change that occurs in a slowly hydrating specimen (Figure 8).

ACKNOWLEDGMENT

This research was supported by the U.S. Department of Energy through the Solar Energy Research Institute under Contract No. DE-FG02-80CS-84051-A002.

NOTATION

D	= effective Knudsen diffusivity, m^2/s
M	= molecular weight, kg/kmol
P	= pressure, Pa
r	= radius, m
r_e	= effective mean pore radius, m
T	= temperature, K
t	= time, s
V	= volume, m^3
X	= conversion, dimensionless

Greek Letters

τ	= tortuosity factor, dimensionless
ω	= void fraction, dimensionless

Subscripts

eq = equilibrium

LITERATURE CITED

- Ball, M. C., and L. S. Norwood, "Studies in the System Calcium Sulphate/Water: Part 4. Rehydration of Hexagonal CaSO_4 ," *J. Chem. Soc., Farad. Trans. I*, **69**, 169 (1973).
- Bielanski, A., and F. C. Tompkins, "Sorption of Water by Dehydrated Alum Crystals," *Trans. Farad. Soc.*, **46**, 1072 (1950).
- Eckhardt, R. C., P. M. Fichte, and T. B. Flanagan, "Kinetics of Rehydration of Crystalline Anhydrides-Manganous Formate," *Trans. Farad. Soc.*, **67**, 1143 (1971).
- Eckhardt, R. C., and T. B. Flanagan, "Anisotropic Solid-State Reaction," *Trans. Farad. Soc.*, **60**, 1289 (1964).
- Flanagan, T. B., "Dehydration Studies of Lead Styphnate Monohydrate," *Trans. Farad. Soc.*, **55**, 114 (1959).
- Flanagan, T. B., "The Kinetics of Sorption and Desorption of Water Vapor by Lead Styphnate," *Can. J. Chem.*, **44**, 2941 (1966).
- Grodzka, P. G., "Thermal Energy Storage," National Technical Information Service Report No. N76-13592 (Nov., 1975).
- Hume, J., and J. Colvin, "The Dehydration of Copper Sulphate Pentahydrate," *Proc. R. Soc.*, **A132**, 548 (1932).
- Satterfield, C. N., *Heterogeneous Catalysis*, McGraw-Hill New York (1980).
- Spencer, W. D., and B. Topley, "Reaction Velocity in the System $\text{Ag}_2\text{CO}_3 \rightleftharpoons \text{Ag}_2\text{O} + \text{CO}_2$," *Trans. Farad. Soc.*, **27**, 94 (1931).
- Stanish, M. A., and D. D. Perlmutter, "Salt Hydrates as Absorbents in Heat Pump Cycles," *Solar Energy*, **26**(4), 333 (1981).
- Stanish, M. A., and D. D. Perlmutter, "Kinetics and Transport Effects in the Dehydration of Crystalline Potassium Carbonate Hydrate," *AIChE J.*, **29**, 806 (Nov., 1983).
- Triollier, M., and B. Guilhot, "The Hydration of Calcium Sulphate Hemihydrate," *Cem. Concr. Res.*, **6**, 507 (1976).

Manuscript received May 27, 1982; revision received November 18, and accepted January 31, 1983.

Oxidative Absorption of H_2S and O_2 by Iron Chelate Solutions

Hydrogen sulfide is oxidized to elemental sulfur by ferric ion chelated with nitrilotriacetic acid (NTA) in aqueous solution at pH 3.5 to 4.5. The reaction appears to be fast relative to gas- and liquid-phase diffusion, and the transfer of H_2S from a gas stream is correlated well by the theory of absorption with instantaneous chemical reaction. The ferrous ion formed in this reaction may be reoxidized with oxygen absorbed from a stream of air. The presence of NTA catalyzes the reaction of O_2 and Fe^{2+} in the same pH range, and diffusion is again controlling. Design calculations based on laboratory data for both absorption steps show that cocurrent gas-liquid contactors are advantageous for achieving high reaction rates (e.g., ~99.99% H_2S removal), high gas velocities (10 to 20 m/s), low pressure drops [1 to 3 kPa (10 to 30 $\text{cm H}_2\text{O}$)], and moderate column heights (10 to 15 m).

D. W. NEUMANN and

SCOTT LYNN

Department of Chemical Engineering
University of California
Berkeley, CA 94720

SCOPE

Hydrogen sulfide is a contaminant in many industrial gas streams that must be removed more or less completely for reasons of safety, environmental protection, and/or processability. A number of processes have been introduced commercially that are based on the oxidative absorption of H_2S . In most cases the

oxidizing agent is dissolved in an aqueous solution at pH 6 or higher. The desired action is to convert the H_2S to elemental sulfur while converting the oxidizing agent to a soluble reduced form that can be reoxidized with air. Ideally, both reactions should be effectively instantaneous. However, many of the

commercially available processes suffer from relatively slow kinetics for both the H_2S -oxidation and the regeneration reactions. Operation is above pH 6 in part to allow H_2S to be absorbed by an acid-base reaction and in part to improve the kinetics of regeneration with air. In this pH range, part of the sulfur is overoxidized to sulfate ion and other species, which necessitates continual pH adjustment and treatment of a purge stream.

CONCLUSIONS AND SIGNIFICANCE

The absorption of H_2S by $\text{Fe}^{3+}\cdot\text{NTA}$ and of O_2 by $\text{Fe}^{2+}\cdot\text{NTA}$ was studied experimentally in a small wetted-wall column. The flows were cocurrent, the temperature was 60 to 65°C, the pH was 3.9 to 4.1, and Re_L was 3,334 in all runs. Both gases were diluted with nitrogen. The data obtained were in good agreement with a model based on absorption with instantaneous, irreversible chemical reaction: the enhancement factor, $E \equiv k_L/k_L^0 = 1 + B^0/zA^*$, allowed quite well for variations in surface concentration of the absorbing species (A^*) of a factor 10 and for variations in the dissolved reactant concentration (B^0) of a factor of 4. The calculated values of E varied by a factor of 7. During these runs, in which hydrodynamic conditions were

Lynn and Dubs (1981) established that the reaction between H_2S and Fe^{3+} chelated with nitrilotriacetic acid (NTA) is rapid at pH 3.5 to 4.5; that overoxidation of sulfur is virtually eliminated at this pH; and that NTA catalyzes the autoxidation of Fe^{2+} even under these relatively acidic conditions. The goal of this study was to determine the relative importance of reaction kinetics and diffusion in the oxidative absorption of H_2S and O_2 by NTA-chelated Fe^{3+} and Fe^{2+} respectively.

kept relatively constant, the physical mass-transfer coefficient, k_L^0 , varied by less than a factor of two and was consistent with a value calculated from the penetration theory for laminar flow of the liquid.

The data were used to size an absorber-regenerator system for producing 10 Mg S/day (11 short ton S/day) by reducing the H_2S content of a gas from 1% to 1 ppm, taking advantage of the characteristics of cocurrent absorbers. To avoid scaling up the laboratory results by a factor of 800,000, one might wish to build and operate a prototype of intermediate size. The method of scale-up presented here would also be useful in the design of such a prototype.

INTRODUCTION

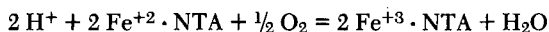
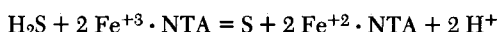
Need for H_2S -Removal Technology

The problem of removing hydrogen sulfide from industrial process streams has existed for over 100 years. That such recovery was and is necessary results from the highly toxic and odorous nature of the gas, which is well documented. Furthermore, recent concern for the environment has yielded stringent restrictions concerning the release of H_2S to the atmosphere. In California, for example, present regulations limit the acceptable ground-level H_2S concentration to 0.06 ppm for three minutes and to 0.03 ppm averaged over one hour (Air Pollution and the San Francisco Bay Area, 1977). It is in response to these strict standards that a variety of processes employing a wide range of technologies have been developed.

The great number and variety of H_2S -removal processes prevents their delineation here. They are discussed in detail in several excellent reviews (for example, Ferguson, 1975; Kohl and Riesenfeld, 1979). Among the most popular approaches is the liquid-phase oxidation of H_2S to elemental sulfur. While many of these schemes are currently in use, a particularly successful one, the Stretford process, uses vanadate ion to oxidize the H_2S . The solution is regenerated by contacting it with air. Addition of anthraquinone disulfonic acid facilitates the latter step. The reactions are carried out in the pH range 7 to 8.

Present Work

The process studied in this work uses ferric iron chelated with nitrilotriacetic acid (NTA) to oxidize the H_2S . Air is employed to regenerate the solution:



The NTA serves two functions: to solubilize the ferric ion, preventing precipitation of the hydroxide at the pH of operation, and to catalyze the reaction of Fe^{+2} with O_2 . The use of NTA allows operation in the pH range of 3.5 to 4.5, which is significantly more acidic than that used in the Stretford process. The acidity prevents the formation of sulfox compounds such as thiosulfate (Lynn and Dubs, 1981). This work was undertaken to determine the rate-

limiting steps in the reactions above, both of which are effectively irreversible.

THEORY

Background Theory for Absorption with Chemical Reaction

In absorption with chemical reaction a molecule, A , is absorbed into a liquid where it reacts with species B according to $A + zB \rightarrow \text{products}$. The reaction may be fast or slow, reversible or irreversible, and of any general order. The overall process can be thought of as occurring in three steps:

1. Diffusion of A from the bulk of the gas phase to the gas-liquid interface and dissolution to form a solution so that gas and liquid are in physical equilibrium at the interface.
2. Diffusion of A from the interface into the liquid.
3. Diffusion of B from the bulk toward the interface and reaction between A and B .

Actually steps 2 and 3 are not necessarily discrete. Often the diffusion and reaction phenomena occur in the same region in the liquid (i.e., near the interface) and thus must be considered simultaneously. The presence of a chemical reaction can significantly distort the concentration profile of A , increasing its gradient and hence accelerating the rate of absorption relative to physical absorption.

The effect of the reaction on the rate of mass transfer is characterized by defining an enhancement factor (Danckwerts, 1970)

$$E \equiv k_L/k_L^0 \quad (1)$$

Thus the rate (or flux) of absorption becomes

$$\begin{aligned} N_A &= k_L(A^* - A^0) \\ &= k_L^0 E(A^* - A^0) \end{aligned} \quad (2)$$

The explicit form of the enhancement factor depends on the rate and order of the reaction and involves solution of the diffusion equations subject to an appropriate model of the liquid-phase hydrodynamics. Danckwerts (1970) presents an excellent review of some of the models used and the results obtained by various investigators.

Concurrent Flow

While the vast majority of columns employed in industry are run countercurrently, there are instances in which the cocurrent configuration is advantageous. In fact, any operation in which only a single equilibrium stage is required may be effectively carried out with cocurrent flow.

Consider for example the case of absorption of a component, A, from a gas phase into a liquid phase where A is consumed by a fast, irreversible chemical reaction with a second component, B. Here complete absorption can be accomplished in a single equilibrium stage, since reaching equilibrium corresponds to complete removal of A provided excess B is present.

Furthermore, the flow rates in cocurrent flow are limited only by the applied pressure gradient in the column and not by flooding as in countercurrent flow. Thus for diffusion-controlled absorption with reaction, cocurrent flow is advantageous because greater turbulence and hence higher k_L^o values can be achieved with the higher velocities attainable in cocurrent operation. This also means that greater gas and liquid throughputs can be used than in countercurrent columns of similar dimensions operated with similar pressure drops.

Absorption with Reaction in a Wetted-Wall Column

For the case of absorption from a gas phase flowing cocurrently to a liquid stream in a wetted-wall column, the rate of absorption is as defined by Eq. 2. Furthermore, since the interfacial area of a wetted-wall column is approximately πDh , the expression can be rearranged to give

$$N_A = q/\pi Dh = k_L(A^* - A^o) \quad (3)$$

If it is assumed that the reaction is fast and irreversible, $A^o = 0$. Thus solving for the effective mass-transfer coefficient gives

$$k_L = q/\pi DhA^* \quad (4)$$

To determine the effect of the presence of an appreciable rate of reaction on the effective mass transfer, one can compare k_L to a theoretical physical mass-transfer coefficient calculated from the Higbie penetration model. Analysis by this method for wetted-wall columns yields (Sherwood et al., 1975)

$$k_L^o = 2\sqrt{(\mathcal{D}/\pi t)} \quad (5)$$

The exposure time of an element of surface in laminar flow is (Danckwerts, 1970)

$$t = (2h/3)(3\mu/g\rho_L)^{1/3} (\mu/Q_L)^{2/3} \quad (6)$$

Note that these expressions indicate that the mass-transfer coefficient k_L^o depends inversely on the square root of height of the column. In general this will not be true for industrial-scale columns because the effect of liquid-phase turbulence on mixing has been ignored. The turbulent eddies tend to cause continual replacement of the surface and thus the contact time is determined by the rate at which the surface is renewed rather than the time it takes the surface layer of liquid to flow down the column. As a result, k_L^o reaches a constant value for column heights greater than a few centimeters.

Mass-Transfer Coefficients from Measurements of Absorption with Instantaneous Reaction

H₂S Absorption. For a wetted-wall or packed column it is possible to derive expressions relating mass-transfer coefficients to column height that account explicitly for the effect of chemical reaction on the rate of absorption. If the reaction is irreversible and sufficiently fast, the bulk equilibrium concentration of A will be reduced to zero. A differential mass balance over a section of column then gives (Danckwerts, 1970)

$$N_A adh = -LdB^o/z = k_L^o aEA^*dh \quad (7)$$

Furthermore, assuming that the reaction is instantaneous allows

one to derive the form of the enhancement factor using the penetration model. Letting $\mathcal{D}_A = \mathcal{D}_B$ (this is suggested as a first approximation since \mathcal{D}_B , the diffusivity of chelated iron, is difficult to estimate), one has (Danckwerts, 1970)

$$E = 1 + B^o/za^* \quad (8)$$

Note that the criterion of irreversibility means that $A^o = 0$.

To determine the value of A^* in terms of B^o , a mass balance is carried out over a section of the column—i.e., for cocurrent flow

$$(y_A^T - y_A)G = L(B_T^o - B^o)/z \quad (9)$$

Thus, assuming that Henry's law applies and that there is negligible gas-phase resistance to mass transfer (see discussion below)

$$A^* = \alpha P_A = \alpha P_t y_A = \alpha P_t \left[y_A^T - \frac{(B_T^o - B^o)}{zG_{ave}} \right] \quad (10)$$

Substituting Eqns. 8 and 10 into Eq. 7 and rearranging yields

$$\begin{aligned} \frac{k_L^o ah}{L} &= \int_{B_B^o}^{B_T^o} \left[\alpha P_t \left(zy_A^T - \frac{L}{G} B_T^o \right) + (\alpha P_t + 1) B^o \right]^{-1} dB^o \\ &= \frac{1}{\gamma} \ln \left[\frac{(\gamma B_T^o + K)}{(\gamma B_B^o + K)} \right] \end{aligned} \quad (11)$$

where

$$\gamma \equiv 1 + \alpha P_t \frac{L}{G}$$

$$K \equiv \alpha P_t \left(zy_A^T - \frac{L}{G} B_T^o \right)$$

Finally

$$k_L^o a = \frac{L}{h\gamma} \ln \frac{(\gamma B_T^o + K)}{(\gamma B_B^o + K)} \quad (12)$$

The liquid-phase physical mass-transfer coefficient can thus be calculated from measurements of the bulk concentration of reactant B^o at the top and bottom of the column and a knowledge of the experimental parameters and the physical properties of the system.

Oxygen Absorption. To analyze the absorption of O₂ and subsequent reaction with Fe²⁺ in a wetted-wall column, the miniplant used in this work was treated as a batch absorber with the contacting limited to the absorption column. During a given run the depletion of Fe²⁺ in the liquid inventory was monitored as a function of time by taking periodic samples of the liquid leaving the column.

When the reaction is fast and irreversible, a mass balance gives

$$V_s \frac{dB_B^o}{dt} = Q_L(B_T^o - B_B^o) = z(y_A^T - y_A^B)Q_G \quad (13)$$

Equation 13 is valid for the conditions of substantial backmixing within the liquid circulation loop that prevailed in this system.

Assuming instantaneous reaction and $\mathcal{D}_A = \mathcal{D}_B$ (i.e., diffusivity of O₂ in solution is roughly equal to that of chelated Fe²⁺), Eq. 12 applies. Furthermore, for O₂ absorption $A^* \ll 1$ so that

$$E_{O_2} \approx B^o/za^* \quad (14)$$

Thus from measurements of the bulk concentration of B^o as a function of time, the physical mass-transfer coefficient for the absorption of A can be calculated. For example, determination of the bulk concentration of ferrous ion with time allows one to determine the value of $k_L^o a$ for absorption of oxygen in a wetted-wall or packed column.

Effect of Gas-Phase Resistance

In the cases discussed above it has been assumed that the gas-phase resistance to mass transfer is negligible. However, if this

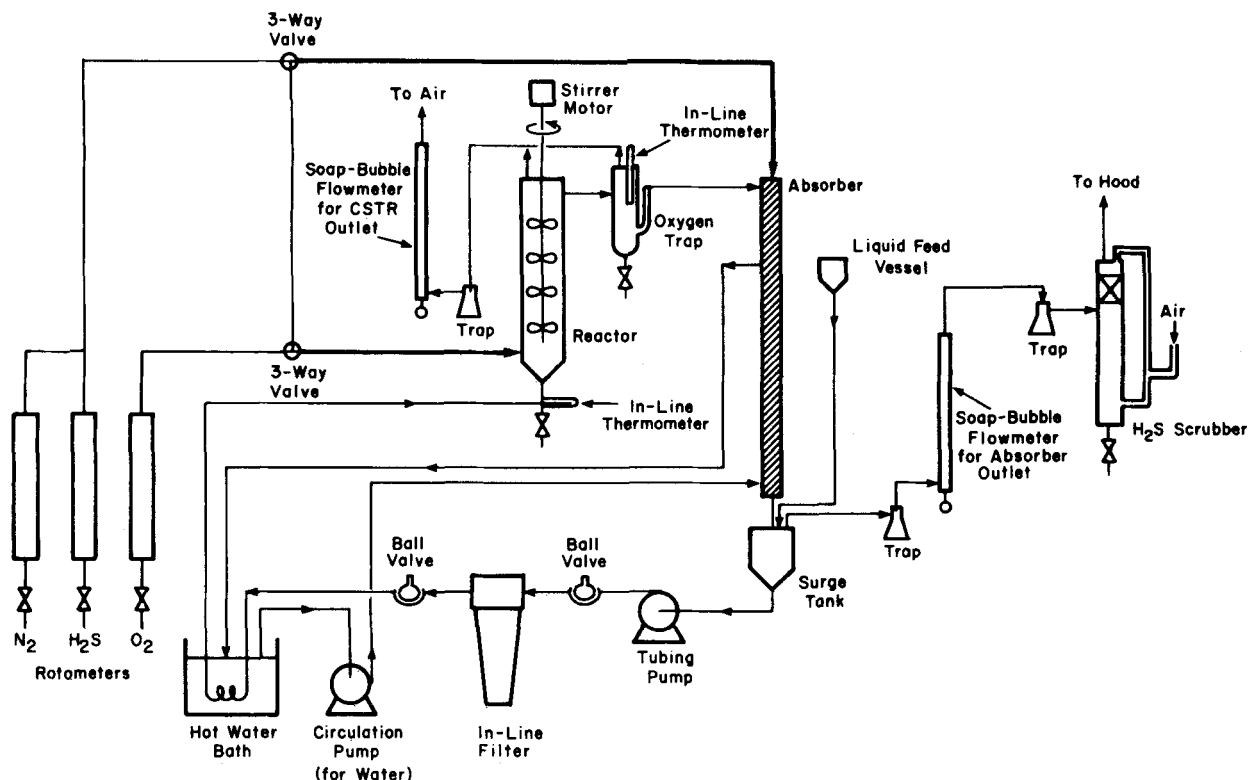


Figure 1. Laboratory apparatus.

resistance becomes sufficiently great, then the rate of absorption no longer depends on the liquid-phase mass-transfer coefficient and the enhancement due to reaction. Consider the case of absorption with instantaneous irreversible reaction, for which the rate expression (using Eq. 8) is

$$N_A = k_L^o(A^* + B^o/z) = k_G P_t(y_A - y_{A_i}) \quad (15)$$

If $B^o \gg A^*$ (i.e., dilute gas stream, sparingly soluble gas, and/or concentrated reactant in liquid), then

$$N_A = k_L^o B^o/z = k_G P_t(y_A - y_{A_i}) \quad (16)$$

Thus

$$y_{A_i} = \frac{k_G P_t y_A - k_L^o B^o/z}{k_G P_t} \quad (17)$$

This indicates that the interfacial concentration y_{A_i} becomes zero when $k_G P_t y_A = k_L^o B^o/z$. Dissolved B then diffuses to the surface and reacts with A as fast (in chemical equivalents) as A reaches the surface by diffusion through the gas.

Above the point where y_{A_i} reaches zero (for a cocurrent down-flow absorber) gaseous A can diffuse to the interface faster than the reaction in the liquid can consume it. The rate of absorption is then entirely controlled by liquid-phase diffusion. The surface concentration, A^* , is maintained by diffusion of A through the gas and Eq. 12 can be used to find the absorber height. Rearranging Eq. 12 and substituting G for L by employing the mass balance (Eq. 9) gives

$$h_I = G \left[\frac{y_A^T - y_A^I}{B_T^o - B_I^o} \right] \frac{z}{k_L^o a \gamma} \ln \left[\frac{\gamma B_T^o + K}{\gamma B_I^o + K} \right] \quad (18)$$

For flow in a wetted-wall column, where $a = 4/D$, Eq. 18 becomes

$$h_I = \frac{DG}{4k_L^o \gamma} \left[\frac{y_A^T - y_A^I}{B_T^o - B_I^o} \right] \ln \left[\frac{\gamma B_T^o + K}{\gamma B_I^o + K} \right] \quad (19)$$

Below the point at which $y_{A_i} = 0$ the process is entirely gas-phase controlled and the rate of absorption is equal to $k_G a P_t y_A$. The interfacial concentration of A remains zero throughout the rest of the column because B can diffuse to the surface and react with A much faster than A can diffuse from the bulk gas to the interface.

It should be noted once more that this analysis is for an instantaneous, irreversible reaction.

One can estimate gas-phase mass-transfer coefficients for wetted-wall columns from the Chilton-Colburn analogy, (Foust et al., 1960).

$$k_G = \frac{G f_g}{8 P_t (1 - y_A)_{LM} Sc^{2/3}} \quad (20)$$

The design equation for diffusion controlled by gas-phase resistance is obtained by substituting Eq. 20 into Eq. 16, simplifying, and noting again that for a wetted-wall column $a = 4/D$.

$$h_{II} = \frac{2 D Sc^{2/3}}{f_g} \ln \left[\frac{y_A^I}{y_A^B} \right] \quad (21)$$

EXPERIMENTAL EQUIPMENT AND PROCEDURES

Miniplant

The experimental apparatus (miniplant) used in this investigation was that built by Kükner (1980), Figure 1. Operation of the equipment is straightforward. The system is filled with a solution of iron-chelate which flows from the liquid feed vessel into the surge tank. Circulation is provided by a pump. The filter and heat exchanger serve respectively to remove sulfur formed in the process and to maintain a solution temperature of 60 to 65°C. When required, a high fraction of Fe^{3+} is produced by oxidizing Fe^{2+} in the solution with pure O_2 in the stirred-tank reactor.

For this work, a turbulent-flow wetted-wall column was used as the absorber. The gas flow rates into the system were measured with rotameters, while the outflows were monitored with bubble flowmeters. Various mixtures of H_2S/N_2 or O_2/N_2 were fed to the absorber by switching the three-way valves.

All of the experiments presented here were performed with approximately 0.10 M iron (derived from $FeSO_4 \cdot 7H_2O$) and 0.11 M NTA in water at pH = 3.9 to 4.1 in the system unless otherwise noted. Additional details are given by Neumann (1981).

Experiments with Turbulent Flow in a Wetted-Wall Column

The apparatus used as the absorber in these experiments was a 6-mm I.D. tube (Figure 2). The cross section of the tube was small to obtain superficial

TABLE 1. ABSORPTION OF H₂S BY IRON-NTA SOLUTION IN A WETTED-WALL COLUMN

I.D. = 6 mm h = 303 mm a = 667 m ² /m ³		$O_L = 7.83 \text{ mL/s}$ $L = 0.277 \text{ m}^3/\text{m}^2\cdot\text{s}$ $Re_L = 3334$		$P_t = 101 \text{ kPa}$ $t = 60^\circ \text{ to } 65^\circ \text{C}$ $pH = 3.9 \text{ to } 4.1$		
V_G (m/s)	y_{H_2S}	$[\text{Fe}^{3+}]_T$ (kmol/m ³)	$\Delta[\text{Fe}^{3+}]^{**}$ (kmol/m ³)	$k_L a$ (s ⁻¹)	E	k_L^0 (m/s)
0.71	0.0903	0.0817	0.0110	1.16	9.5	183×10^{-6}
0.99	0.0665	0.0853	0.0105	1.47	13.1	168×10^{-6}
1.13	0.0586	0.0895	0.0099	1.57	15.4	153×10^{-6}
1.13	0.0586	0.0895	0.0105	1.57	15.4	163×10^{-6}
1.24	0.0541	0.0772	0.0097	1.69	14.4	175×10^{-6}
1.43	0.0461	0.0859	0.0095	1.89	18.5	153×10^{-6}
1.51	0.0442	0.0696	0.0086	1.81	15.9	171×10^{-6}
1.65	0.0403	0.0869	0.0084	1.90	21.3	133×10^{-6}
1.73	0.0387	0.0683	0.0084	2.01	17.6	171×10^{-6}

* The corresponding values of G and Re_G vary proportionately from 0.026 to 0.063 kmol/m²s and from 253 to 590, respectively.

** $\Delta[\text{Fe}^{3+}] = [\text{Fe}^{3+}]_T - [\text{Fe}^{3+}]_B$

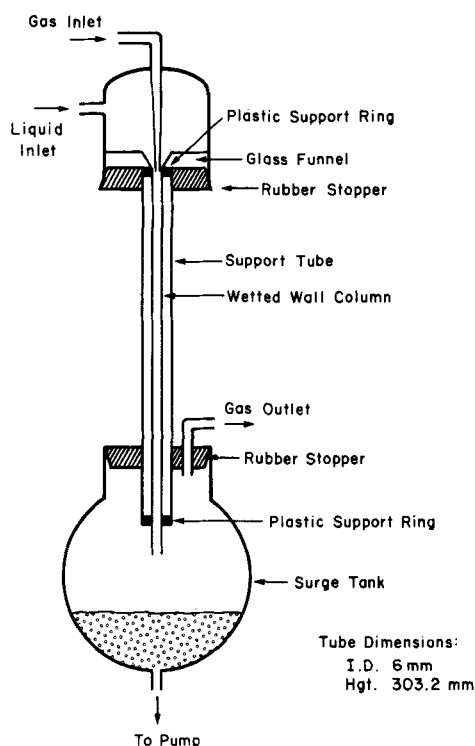


Figure 2. Wetted-wall column.

gas velocities sufficient to produce considerable shear at the gas-liquid interface from the limited laboratory flow rates. All runs were performed with enough gas flow to force the liquid to flow down the column walls around a gas core. This minimized any capillary effects arising from the small diameter of the tube. Separate procedures for measuring the rates of absorption of H₂S and of O₂ were devised.

Absorption of H₂S. In these experiments samples of solution were taken from the surge vessels above and below the column and analyzed for [Fe³⁺] by the method described below (square brackets indicate concentration). To minimize any effect of mixing in the surge flasks, sampling was undertaken only after system operation was at steady state—i.e., constant oxidation potential was maintained at the top of the absorber by introducing excess oxygen to the stirred-tank reactor.

Various flow rates of H₂S and N₂ were fed to the absorber, while the liquid flow was held constant at 470 cm³/min. From the change in [Fe³⁺] the rate of absorption of H₂S could be determined as a function of the conditions employed.

Absorption of O₂. Since the absorption of oxygen depends on [Fe²⁺], the iron in the solution was reduced by reaction with H₂S to ensure a high level of [Fe²⁺] at the beginning of a run. With the plant operating at steady temperature the H₂S flow was stopped, and an approximately 20% O₂ and 80% N₂ mixture (i.e., roughly air composition) was introduced into the

absorption column. Samples of solution were removed from the surge tank at various times and analyzed for [Fe³⁺] (and [Fe²⁺] by difference from the known total [Fe]) to indicate the transient absorption of O₂.

Analytical Procedure for Determining [Fe³⁺] and [Fe²⁺]

In some of the experiments it was necessary to determine directly the concentrations of ferrous and/or ferric iron. To determine [Fe³⁺] a sample was acidified, treated with excess KI, and allowed to stand in the dark for 5 to 10 minutes. The sample was then titrated with standard Na₂S₂O₃ to the starch endpoint.

To determine [Fe²⁺], samples were titrated with standard K₂Cr₂O₇. The end point was observed as a sudden change in the oxidation potential.

Titration for both Fe²⁺ and Fe³⁺ makes it possible to determine accurately the total iron content of the solution. Then analyzing for either Fe³⁺ or Fe²⁺ during a run allows specification of the other.

EXPERIMENTAL RESULTS

Hydrogen Sulfide Absorption

From the experimental observation that sulfur forms immediately upon contact of H₂S with Fe³⁺-NTA solution, it was hypothesized that the reaction is instantaneous relative to diffusion. To test this hypothesis Eq. 12 was applied with $B = [\text{Fe}^{3+}]$ and $\alpha = 0.523 \times 10^{-6} \text{ kmol/m}^3\cdot\text{Pa}$ for H₂S in water at 60°C. This value, from Perry and Chilton (1973), is probably high because of the salting-out effect of the iron chelates. The lower pH of these solutions would have little effect on the solubility of H₂S since it is quite a weak acid. The results for various runs analyzed by this method are given in Table 1. Values of k_L^0 were obtained from $k_L^0 a$ coefficients by dividing by the nominal interfacial area per unit volume ($a = 4/D = 667 \text{ m}^{-1}$) for the wetted-wall column.

Also included in the table is an approximate value of $k_L a$, calculated using the enhancement factor at the top of the column

$$E_{H_2S} = 1 + \frac{[\text{Fe}^{3+}]_T}{2\alpha_{H_2S}y_{H_2S}P_t} \quad (22)$$

In these runs the flow rate of H₂S was kept constant at 1.68 mL/s and G was increased by increasing the flow rate of N₂ from 17.0 to 41.8 mL/s. Thus, as gas velocity rose y_{H_2S} dropped. As is shown in Table 1, as V_G increased the effective mass transfer coefficient, $k_L a$, also rose. However, the physical mass transfer coefficient, k_L^0 , was found to be independent of the gas-phase Reynolds number (or flow rate) over the range considered, Figure 3. Thus all of the variation in $k_L a$ is accounted for by the enhancement factor, Eq. 22. The variation in the gas flow employed was apparently not sufficient to cause an appreciable change in the liquid-phase mass transfer characteristics. Note that the range of Re_G is fairly small, and Sherwood et al. (1975) indicate that the effect of gas drag on liquid turbulence is not great at commonly encountered gas rates.

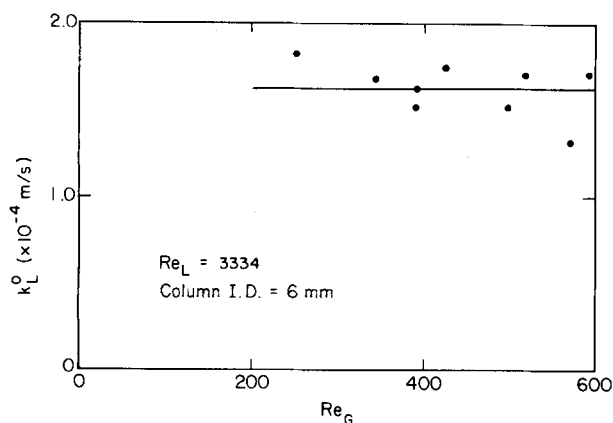


Figure 3. Variation of k_L^0 for H_2S absorption in wetted-wall column.

It is of interest to use Eq. 5 together with the experimentally determined value of k_L^0 to calculate an effective residence or contact time for the surface elements in the liquid film, and to compare this value with that obtained from Eq. 6, which is applicable for a semiparabolic velocity profile. Letting $\mathcal{D}_{H_2S} = 3.8 \times 10^{-9} \text{ m}^2/\text{s}$ and $k_L^0 = 168 \times 10^{-6} \text{ m/s}$, Eq. 5 gives $t = 0.17 \text{ s}$. The contact time for an element of liquid surface in the column, calculated from Eq. 6 for a parabolic velocity profile, is 0.20 s. The agreement between the experimental results and simple penetration theory is thus good. Because the effect of turbulence on the effective contact time is small, the conclusion that the value of k_L^0 depends on surface renewal, and hence is independent of column length, is indicated but not thoroughly demonstrated.

The theory for absorption with chemical reaction predicts that the net rate of absorption is independent of the gas-phase concentration of H_2S . This means that a loss in gas-phase driving force (i.e., reduced A^*) is compensated for by a corresponding increase in the enhancement factor because of the instantaneous reaction. That this effect is at play is shown in Table 1 by the relatively small change in $\Delta[\text{Fe}^{3+}]$ as $y_{H_2S}^T$ drops with increasing gas velocity. As long as the reaction zone is within the liquid, past the interface, the rate of absorption of A is governed solely by the rate at which B can diffuse to that zone. The data reported in Table 1 support this prediction and thus appear to indicate that the reaction between H_2S and Fe^{3+} -NTA at pH 3.9 to 4.1 and 60° to 65°C is effectively instantaneous.

Oxygen Absorption

Preliminary experiments with pure O_2 indicated that the absorption and subsequent reaction with Fe^{2+} is also probably diffusion-controlled. Assuming that the reaction is instantaneous, one can apply Eq. 12 to the transient absorption of O_2 in a wetted-wall column. The values of B_T^0 are obtained by analyzing samples taken from the surge tank periodically for Fe^{2+} concentration (B_B^0) and using Eq. 13 to estimate the change in $[\text{Fe}^{2+}]$. The variation of $[\text{Fe}^{2+}]$ with time for the surge-pot samples for three separate runs is shown in Figure 4. The linearity of the time-dependence of the data plotted in this form is predicted by the model for absorption with instantaneous chemical reaction if the change in y_{O_2} in the gas flowing through the column is small. From the data in Figure 4 and the relationship given in Eq. 13 it can be calculated that y_{O_2} changes 10% or less, as does $[\text{Fe}^{2+}]$, in any given pass through the column.

The values of k_L^0 calculated for various gas flows are given in Table 2. In contrast to the H_2S results, these data show an increase in mass transfer coefficient with gas flowrate. This may be caused by the shear on the gas-liquid interface or by some other feature which is not important in H_2S absorption. To determine whether this effect is genuine or simply an artifact of the experimental method would require further investigation. However, since the values of k_L^0 for O_2 are of the same magnitude as that for H_2S , they represent a useful first approximation for the mass-transfer be-

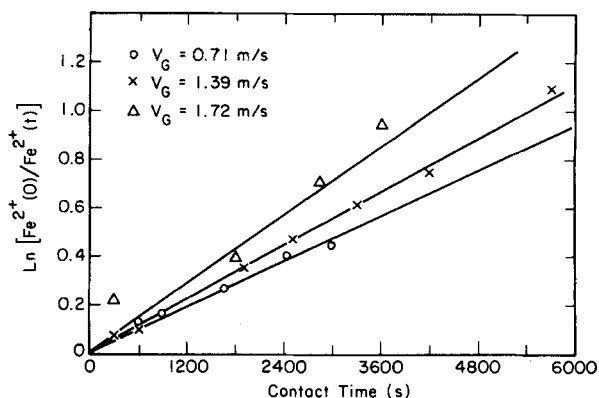


Figure 4. Decrease of $[\text{Fe}^{2+}]$ with time during O_2 absorption.

TABLE 2. MASS TRANSFER COEFFICIENTS FOR ABSORPTION OF OXYGEN BY IRON-NTA SOLUTION IN A WETTED-WALL COLUMN*

V_G^{**} (m/s)	$y_{O_2}^T$	$[\text{Fe}^{2+}]$ (kmol/m ³)	E_{ave}	k_L^0 (m/s)
0.80	0.215	0.0665 to 0.0427	73	75×10^{-6}
1.58	0.201	0.0702 to 0.0236	63	90×10^{-6}
1.99	0.201	0.0531 to 0.0207	53	120×10^{-6}

* Physical and liquid flow parameters same as those in Table 1.

** G and Re_G vary proportionately from 0.021 to 0.073 kmol/m²-s and from 314 to 783, respectively.

havior of this system. It should be noted that the values of E_{ave} listed in Table 2 are averages of values that vary significantly during any given run, as is apparent from examination of Eq. 14.

DESIGN CONSIDERATIONS AND CALCULATIONS

The experimental data presented above can perhaps best be placed in perspective through using them to size the absorbers for a plant of typical feed composition and capacity. The design basis chosen was the removal of 99.99% of the H_2S from a gas stream initially containing 0.010 mole fraction H_2S . Total sulfur production would be 10 Mg/d (11 short ton per day). The corresponding flow rate of a gas having the properties of nitrogen at a pressure of 1 atm and 25°C would be $8.65 \text{ m}^3/\text{s}$ (18,900 standard ft³/min).

H_2S Absorber

The oxidative absorption of H_2S from a gas stream is complicated by the formation of solid sulfur. In a packed column not all of the sulfur formed is swept away by the iron chelate solution; part is deposited on dry areas of the packing where it sticks tenaciously. In a wetted-wall column, however, there are no unlubricated areas and no tendency for sulfur to deposit has been observed. A feasible absorber design would thus be a number of wetted-wall columns operated in parallel. The conceptual design that is proposed here consists of a bundle of 50-mm (2-in.) stainless-steel tubes fixed in tube sheets top and bottom so as to resemble a heat exchanger minus its shell. Headers top and bottom would serve to feed and to disengage the concurrently flowing liquid and gas streams.

The flow rate of liquid and gas in the absorber are linked through the reaction stoichiometry and the changes in H_2S and Fe^{3+} content that are to occur. The uptake of H_2S is a design parameter. Solubility limits the total iron chelate concentration to about 0.6 kmol/m^3 , so the concentrations of Fe^{3+} at the top and bottom of the H_2S absorber were set arbitrarily at 0.4 and 0.2 kmol/m^3 respectively. (The use of a larger concentration swing would reduce the flow rate of the absorbent but would require greater heights for both the H_2S and the oxygen absorbers, so that optimization

TABLE 3. H₂S ABSORBER DESIGN

Design Parameters	
Gas Flow = 8.65 m ³ /s (18,300 ft ³ /min)	Liquid flow = 35 L/s (555 gal/min)
$y_{\text{H}_2\text{S}}^T = 0.010$ (1%)	$[\text{Fe}^{3+}]_T = 0.40$ kmol/m ³
$y_{\text{H}_2\text{S}}^B = 0.000001$ (1 ppm)	$[\text{Fe}^{3+}]_B = 0.20$ kmol/m ³
Tube Diameter = 50 mm (2 in.)	$P_t = 101$ kPa (1 atm)
	$t = 60$ to 65°C
Flow Characteristics	
$V_G = 15$ m/s	$L = 0.061$ m ³ /m ² ·s
$G = 0.617$ kmol/m ² ·s	$Re_L = 6130$
$Re_G = 49,000$	$\delta = 0.49$ mm
$f_g = 0.083$	$k_L^q = 168 \times 10^{-6}$ m/s
$dP/dx = 220$ Pa/m	$a = 80$ m ⁻¹
$k_G = 72 \times 10^{-9}$ kmol/m ² ·Pa·s	
At $y_i = 0$, $y_{\text{H}_2\text{S}} = 0.0031$ and $[\text{Fe}^{3+}] = 0.26$ kmol/m ³	
Absorber Dimensions	
Number of Tubes	= 293
Tube Bundle Diameter	= 1.2 m (4.0 ft)
h_l (Liquid-Phase Controlled)	= 3.2 m
h_{ll} (Gas-Phase Controlled)	= 2.8 m
Total Height of Tubes	= 6.0 m (20 ft)
Total Pressure Drop	= 1.4 kPa (5.6 in. H ₂ O)

would be required in a more detailed design.) These considerations set the ratio of volumetric flows at 4.1×10^{-3} m³ liquid/m³ gas.

Finally, it was decided arbitrarily to set the pressure drop through the absorber at 1 to 2 kPa (4 to 8 in. of water). Friction factor data for two-phase downward flow of air and water in 50-mm tubes (Chien and Ibele, 1964) were used to estimate both the pressure gradient in a single tube for a selected combination of gas and liquid flows and the value of k_G predicted by Eq. 20. Equations 9, 17, 19 and 21 were then combined to allow estimation of the length of tube required to achieve the desired H₂S removal at the selected flowrates. The combination of flows for which the pressure drops would be 1 to 2 kPa in the length needed to achieve the desired H₂S removal was found by trial and error. The parameters for this design are summarized in Table 3.

It should be noted that rather rough approximations are made in obtaining the value of k_L^q and k_G listed in Table 3. Values of k_L^q obtained in a 6-mm tube at $Re_L = 3,334$ are used in a 50-mm tube at $Re_L = 6,130$. This approximation should be conservative, since increasing Re_L should increase the turbulence in the liquid film and enhance k_L^q . Similarly, it is not certain that the Chilton-Colburn analogy, used to obtain a value for k_G , is applicable to two-phase flow. The maximum uncertainty in k_G is about a factor of 4, which is the ratio of f_g 's with and without liquid flowing cocurrently with the gas. One would clearly want to operate a single-tube prototype of the proposed absorber to obtain data for a detailed design.

O₂ Absorber

The design of the oxygen absorber is simplified by the fact that no solid product is formed. It is likely that one would select a packed column employing a packing with a high porosity, such as Pall rings. However, it is difficult to use the data obtained in this work to predict the mass transfer characteristics for such a packing with any certainty. For this reason, the column will again be assumed to consist of a bundle of tubes of the required length. In contrast to the H₂S absorber, in which flow was restricted to the insides of the tubes, in the O₂ absorber the flow of liquid is assumed to be evenly distributed on both surfaces of each tube. If the total liquid flow is kept the same as for the H₂S absorber, the diameter of the individual tubes is taken as 25 mm, and the value of Re_L is taken as 3,334, then the total number of tubes required will be 538. With a packing density of 60% this bundle of tubes would fit in a column having an inner diameter of 0.75 m (2.5 ft).

Keeping the value of Re_L at 3,334 is equivalent to keeping the rate of flow of liquid per unit perimeter of packing the same for the design as for the laboratory experiments. Under these conditions one might reasonably expect the value of k_L^q to be the same as well.

TABLE 4. OXYGEN ABSORBER DESIGN

Design Parameters	
Air Flow = 0.38 m ³ /s (500 ft ³ /min)	Liquid Flow = 35 L/s (555 gal/min)
$y_{\text{O}_2}^T = 0.20$	$[\text{Fe}^{2+}]_T = 0.40$ kmol/m ³
$y_{\text{O}_2}^B = 0.03$	$[\text{Fe}^{2+}]_B = 0.20$ kmol/m ³
Tube Diameter = 25 mm (1 in.)	$P_t = 101$ kPa (1 atm)
	$t = 60$ to 65°C
Flow Characteristics	
$V_G = 0.6$ m/s (2 ft/s)	$L = 0.080$ m ³ /m ² ·s
$G = 0.023$ kmol/m ² ·s	$Re_L = 3334$
$Re_G = 980$	$k_L^q = 75 \times 10^{-6}$ m/s
	$a = 200$ m ² /m ³
Absorber Dimensions	
Number of Tubes = 538	
Tube Jacket (Column) Diameter = 0.75 m (2.5 ft)	
Diameter of Tubes = 25 mm	
Length of Tube = 3.7 m (12 ft)	
Total Pressure Drop < 0.3 kPa (1 in. H ₂ O)	

The value assumed, 75×10^{-6} m/s, was the lowest of the three values found. The column height required for the desired conversion of Fe²⁺ is 3.7 m (12 ft).

The minimum air flow necessary for the O₂ absorber is set stoichiometrically by the need to oxidize the Fe²⁺ from the feed concentration of 0.4 kmol/m³ to the outlet concentration of 0.2 kmol/m³. An excess of 20% was provided to ensure that liquid-phase diffusion was the rate-controlling step throughout the column. This corresponds to an air flow of 0.30 m³/s (600 ft³/min) for a superficial gas velocity of 0.6 m/s (2 ft/s). The total pressure drop for the air flow is estimated at less than 0.3 kPa (1 in. water).

The design parameters, assumptions, and calculations are summarized in Table 4. Again, it should be noted that this design is based on a scale-up of the laboratory data of about 800,000. It is clear that a pilot plant should be built and operated to test some of the assumptions upon which this design is based.

Design Comparison

One value of a design exercise such as that above is to allow visualization of the plant-scale equipment that would result from suitable scale-up of the laboratory results. A second value is to determine whether that equipment as visualized offers sufficient potential advantage to encourage continued development. It is thus instructive to compare the H₂S and O₂ absorbers for a typical Stretford process plant (Kohl and Riesenfeld, 1979) with those above. This Stretford H₂S-absorber reduces the H₂S content of coke-oven gas from 0.4% to 15 ppm. The superficial gas velocity is 0.44 m/s, the ratio of liquid to gas flows is 0.012 m³/m³, and the column height is 30 m. The Stretford O₂ absorber consists of a tank of liquid 6 m deep into which air is sparged. The superficial air velocity is 0.16 m/s, the liquid/gas flow ratio is 0.24 m³/m³ and the pressure drop for the air is somewhat more than 670 kPa. The designs presented in Tables 3 and 4 compare quite favorably with these Stretford units, which would be a positive factor in the development decision.

CONCLUSIONS

The oxidative absorption of H₂S by Fe³⁺-NTA solution, and of O₂ by Fe²⁺-NTA solution, appears to involve fast, irreversible chemical reactions. As a result, cocurrent flow of gas and liquid in the absorbers can be employed, which leads to compact equipment and low pressure drops. Laboratory data have been used to estimate the size of an absorber-regenerator system for removing 99.99% of the H₂S from a gas stream. The absorber sizes illustrate the compactness of cocurrent absorbers. However, the design represents a scale-up of about 800,000 and clearly needs verification at the pilot-plant scale.

ACKNOWLEDGMENT

This work was supported in part by the Chemical and Process Engineering Div. of the National Science Foundation under Grant DAR-78116899.

NOTATION

a	= interfacial area per unit volume of absorber (m^2/m^3)
A^o	= concentration of A in bulk liquid (kmol/m^3)
A^*	= Concentration of A in the liquid at the interface, in equilibrium with gas at interface (kmol/m^3)
B^o	= Concentration of B in bulk liquid (kmol/m^3)
D	= column or tower diameter (m)
\mathcal{D}	= diffusivity (m^2/s)
E	= enhancement factor, dimensionless, $\equiv k_L/k_L^o$
f_g	= friction factor, dimensionless
g	= gravitational acceleration (m/s^2)
G	= average superficial molar gas velocity ($\text{kmol}/\text{m}^2\cdot\text{s}$)
h	= column height (m)
K	= defined in Eq. 11
k_G	= gas-phase mass-transfer coefficient ($\text{kmol}/\text{m}^2\cdot\text{Pa}\cdot\text{s}$)
k_L	= effective liquid-phase mass-transfer (m/s)
k_L^o	= liquid-phase mass transfer coefficient for physical absorption (m/s)
L	= average superficial liquid velocity ($\text{m}^3/\text{m}^2\cdot\text{s}$)
N_A	= average rate of absorption of species A ($\text{kmol}/\text{m}^2\cdot\text{s}$)
P_A	= partial pressure of A in bulk gas phase (Pa)
P_t	= total pressure (Pa)
q	= rate of absorption (kmol/s)
Q_G	= gas flow rate (kmol/s)
Q_L	= liquid flow rate (m^3/s)
Re_G	= gas-phase Reynolds number, $DV_G\rho/\mu$
Re_L	= liquid-phase Reynolds number, $4Q_L\rho_L/\pi D\mu$
Sc	= Schmidt number, $\mu/\rho\mathcal{D}$
t	= exposure time of an element of liquid surface (s)
V_G	= gas superficial velocity (m/s)
V_s	= total liquid inventory (m^3)
y_A	= Mole fraction of A in the gas phase
z	= number of moles of reactant B reacting with each mole of A

α	= solubility coefficient ($\text{kmol}/\text{m}^3\cdot\text{Pa}$)
γ	= expression defined in Eq. 11
δ	= liquid layer thickness on a pipe wall (m)
μ	= viscosity ($\text{Pa}\cdot\text{s}$)
ρ	= density (kg/m^3)

Subscripts and Superscripts

B	= bottom of column
i	= interface composition or partial pressure
I	= region (or bottom of region) in which liquid-phase diffusion controls
II	= region in which gas-phase diffusion controls
LM	= log mean
T	= top of column

LITERATURE CITED

- "Air Pollution and the San Francisco Bay Area," Bay Area Air Pollution District, 11th Ed. (June, 1977).
- Chien, S.-F., and W. Ibele, "Pressure Drop and Liquid Film Thickness of Two-Phase Annular and Annular-Mist Flows," *J. of Heat Trans., Trans. of ASME*, 87, 89 (1964).
- Danckwerts, P. V., *Gas-Liquid Reactions*, McGraw-Hill, 34, 193, 113 (1970).
- Ferguson, P. A., "Hydrogen Sulfide Removal from Gases, Air and Liquids," Noyes Data Corp. (1975).
- Kohl, A. L., and F. C. Riesenfeld, *Gas Purification*, Gulf Publishing, 3rd Ed., 485 (1979).
- Kükner, G., "Alternative Iron Chelating Agents for Oxidative Absorption of H_2 ," M.S. Thesis, University of California Berkeley (1980).
- Lynn, S., and B. Dubs, "Oxidative Removal of Hydrogen Sulfide from Gaseous Streams," U.S. Patent # 4,278,646 (July, 1981).
- Neumann, D. W., "Oxidative Absorption of H_2S and O_2 by Iron-Chelate Solutions," M.S. Thesis, University of California, Berkeley (1981).
- Perry, R. H., and C. H. Chilton, *Chemical Engineers' Handbook*, 5th Ed., McGraw-Hill, (1973).
- Peters, M. S., and K. D. Timmerhaus, *Plant Design and Economics for Chemical Engineers*, 3rd Ed., McGraw-Hill (1980).
- Sherwood, T. K., R. L. Pigford, and C. R. Wilke, *Mass Transfer*, McGraw-Hill, 154, 205 (1975).

Manuscript received July 20, 1982; revision received January 27, and accepted January 31, 1983.

Computer-Aided Synthesis and Design of Plant Utility Systems

A design synthesis procedure is developed for preliminary design of utility systems. Given known steam sources (waste heat and auxiliary boilers) and sinks (heating, process injection, and driver horsepower needs), the algorithm determines the optimal header pressure levels, the distribution of steam turbines in the network, and the steam flows between all devices so as to maximize the real work recovered from the sources. Any number of pressure levels can be accommodated at only modest increase in computational effort.

T. PETROULAS and

G. V. REKLAITIS

School of Chemical Engineering
Purdue University
West Lafayette, IN 47907

SCOPE

With the growing emphasis on energy conservation in process operation and design, there is a need for efficiency in the design of plant utilities systems and in the integration of the utilities system design with the process-side design. Most of the publications dealing with the synthesis and design of utilities systems

have focused on the balance calculations associated with fixed utility system networks with specified header pressure levels. For instance, Gordon et al. (1978) discuss computerized steam balance calculations; Wilkinson (1979) presents a specialized simulation/design approach for performing steam balances and